Advances in Geosciences, 6, 111–118, 2006
SRef-ID: 1680-7359/adgeo/2006-6-111
European Geosciences Union
© 2006 Author(s). This work is licensed
under a Creative Commons License.

Advances in Geosciences

A study of the sensitivity of ENSO to the mean climate

T. Toniazzo

Hadley Centre for Climate Prediction and Research, Met. Office, Exeter, UK

Received: 8 July 2005 – Revised: 30 September 2005 – Accepted: 28 October 2005 – Published: 9 January 2006

Abstract. We study the dependence of the simulated ENSO on the mean simulated climate in the HadCM3 GCM and attempt to understand its relation with results from intermediate-complexity models (ICMs). Our aim is to bridge an existing gap between results from complex GCMs and from more readily understandable ICMs, and thereby to improve our process-based prediction skills of the potential sensitivity of observed ENSO properties (amplitude, frequency and pattern) to climate change. Although there is a suggestion that surface ENSO processes are dominating the response in HadCM3, our work also shows that the complex changes in simulated climate can have contrasting effects on the ENSO and the net result may not be robust.

1 Introduction

A projection for future changes in the ENSO entails three separate problems: prediction of the 3-D pattern of oceanic warming, of shifts in convective regimes, of the annual cycle etc.; modeling of the consequences for the ENSO; and modeling of the resulting changes in direct and indirect teleconnections of El Niño's or La Niña's. In relation to each of these points, our confidence in the simulations using global circulation models ("GCM"s) is low. Results from different GCMs for anthropogenic greenhouse-forced climate-change scenarios are not consistent with each other (Collins and the CMIP modelling group, 2005; van Oldenborgh et al., 2005[1]; Merryfield, 2005[2]; Guilyardi, 2005[3]). This uncertainty is compounded by model biases for the current climatology and for the current ENSO (including its teleconnections), and by our incomplete physical understanding of the results from GCM simulations.

A step-wise approach to the problem of ENSO change, as outlined above, may therefore be necessary to help placing better-defined (and hopefully more stringent) confidence limits on future projections. Here we address the question of which changes in the climate-mean properties affect the amplitude, the frequency and the pattern of the ENSO, and how. We show some results from the analysis of the ENSO changes between three different steady-state climate integrations of the HadCM3 model (Toniazzo, 2005[4]); we discuss them in the light of ICM modeling and compare them with the results for the ENSO with an intermediate tropical coupled model developed by at IPRC/SOEST (University of Hawai'i at Manoa) by Bin Wang and collaborators (Wang and Li, 1993; Wang, Li and Chan, 1995; Seager et al., 1995; Fu and Wang, 1999).

2 ENSO properties and mean climate in three HadCM3 steady-state integrations

2.1 Change in ENSO-properties and characteristics of El Niño anomalies.

We analysed three long steady-state climate integrations (all without flux corrections) with the HadCM3 model, which are set up as follows:

> LGM: (Hewitt et al., 2001, 2003) has an atmospheric CO_2 concentration of 200 ppm, extended land areas and an orographic and surface-type representation for the Last-Glacial-Maximum Laurentide and Fennoscandian ice-sheets (Peltier, 1994);

Correspondence to: T. Toniazzo
(thomas.toniazzo@metoffice.gov.uk)

[1] van Oldenborgh, G. J., Philip, S., and Collins, M.: El Niño in a changing climate: a multi-model study, Ocean Sci., submitted, 2005.

[2] Merryfield, W. J.: Changes to ENSO under CO_2 doubling in the IPCC AR4 coupled climate models, J. Clim., submitted, 2005.

[3] Guilyardi, E.: El Niño mean state – seasonal cycle interactions in a multi-model ensemble, Clim. Dyn., submitted, 2005.

[4] Toniazzo, T.: The simulation of the El Niño-Southern Oscillation in different equilibrium climates with the HadCM3 model, J. Clim., submitted, #JCL-5384, 2005.

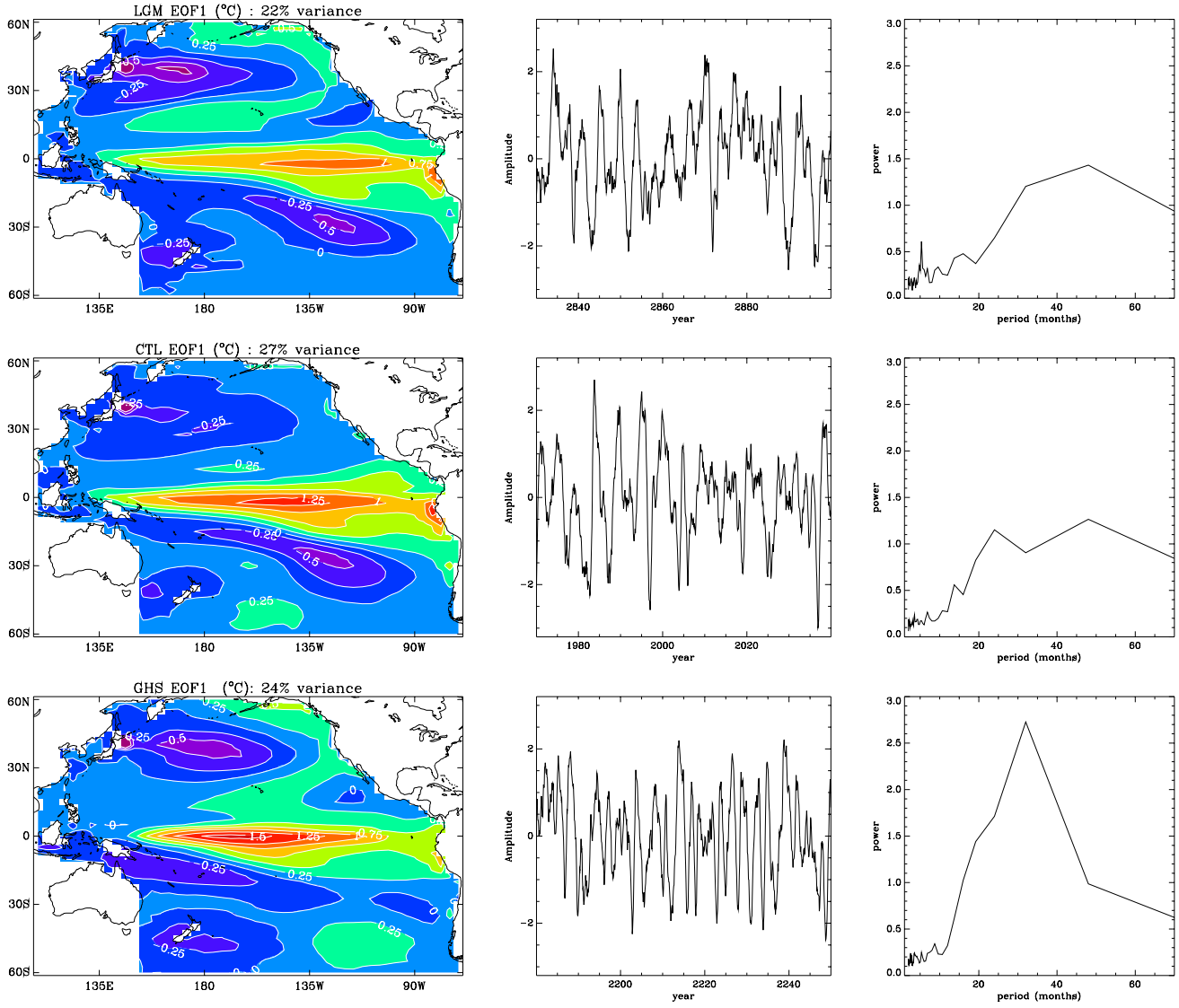

Fig. 1. Patterns, amplitudes and power spectra (from left to right) of the 1st EOFs of tropical-Pacific interannual SST anomalies for the LGM (top), CTL (middle) and GHS (bottom) HadCM3 integrations.

CTL: (Pope et al., 2000) has a CO_2 concentration of 280 ppm, and modern (pre-industrial) land-surface cover and topography;

GHS: (Thorpe, 2004) is identical with CTL but with a four-fold CO_2 concentration of 1120 ppm.

All integrations where carried forward for more than 1000 model-years.

The leading EOF modes (Fig. 1) of tropical-Pacific monthly SST interannual anomalies (henceforth "SSTa"'s) for the three integrations (Toniazzo, 2005[4]) show a systematic shift from a predominantly Eastern-Pacific to a predominantly Central Pacific mode, as well as towards higher frequencies, when going from LGM to CTL and from CTL to GHS. The variance explained by the first EOF is similar in each case, and the standard deviation of zonally integrated Equatorial (5 S–5 N) SST anomalies is also similar. Due to the pattern shift, however, the NINO3 (150 W–90 W) standard deviation progressively decreases, while the NINO4 (160 E–150 W) variability tends to increase (but less significantly); the zonal extent of the SST pattern also appears to contract (Fig. 1), resulting in larger peak SST anomalies for GHS. The power spectra of the standard NINO indices broadly confirm the tendency found for the EOF1 time-series, with increasingly more fractional power at higher frequencies. The oscillation is most regular in GHS, and least in LGM (Toniazzo, 2005[4]). The seasonal distribution of SSTa's (not shown) is similar for the LGM and CTL cases, but in GHS it appears to peak earlier in the year and with a narrower spread (particularly the NINO4 index).

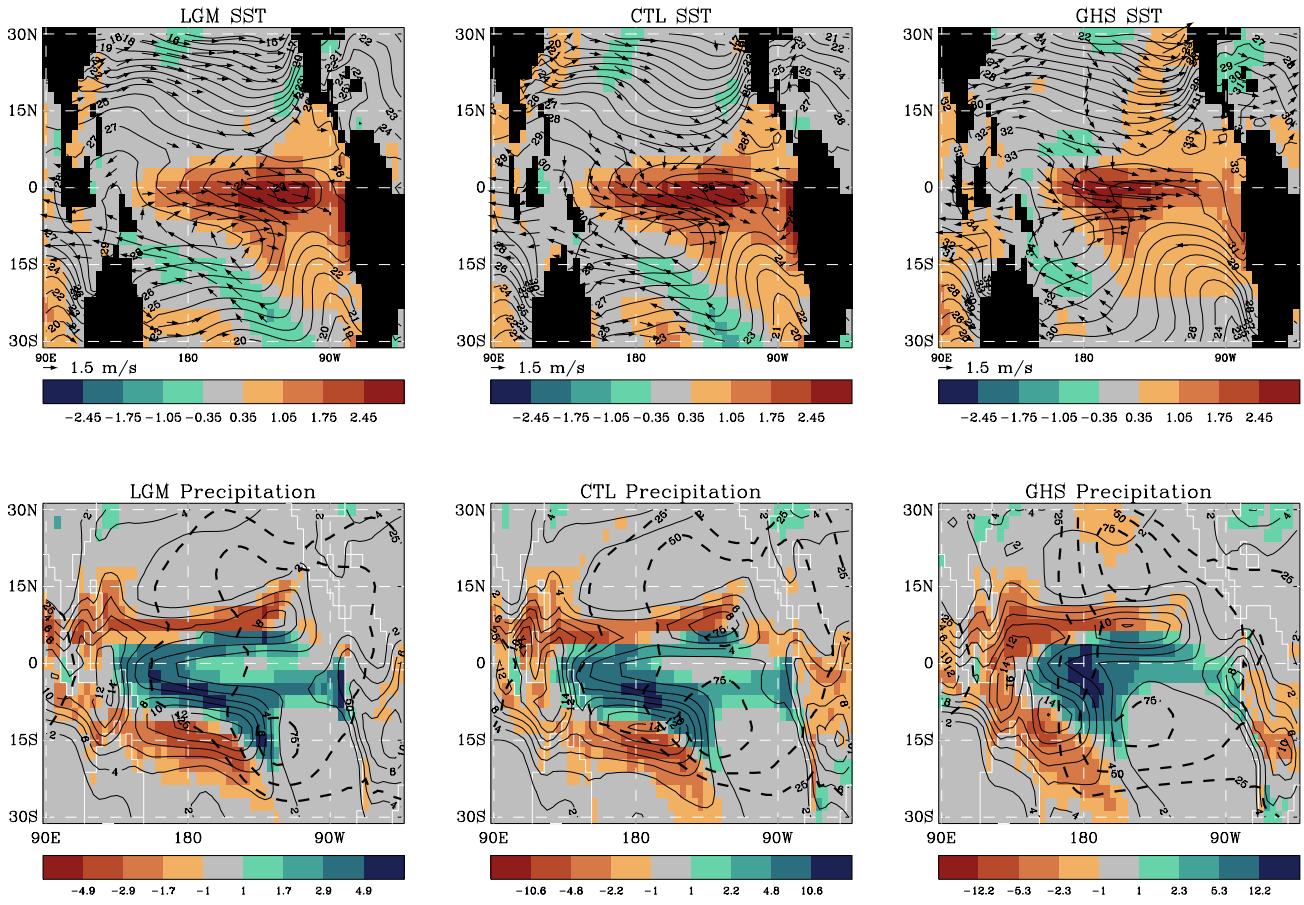

Fig. 2. DJF SST (top) and precipitation (bottom) fields for the three HadCM3 integrations; climatology is shown as solid contours, El Niño anomalies are shown as colours. The arrows in the upper panels represent 850hPa DJF wind anomalies for each case (arrows of magnitude smaller than 1 m/s are not plotted), and the broken contours in the lower panels represent DJF 200 hPa–850 hPa thickness anomalies.

El Niño anomalies in SST, precipitation and windstress, along with DJF climatology, are shown in Fig. 2. The spatial relation between SST and precipitation anomalies differs in the three climate integrations. The maximum SST anomalies change location from near the minimum climatological SSTs in the Eastern Pacific, far from the climatological convective areas, to the central-Western Pacific (an area with a large zonal gradient in climatological SSTs). Almost irrespective of this shift, the largest convective anomalies occur in all cases at the edges of the climatological convective regions, where convection is more easily triggered by SST anomalies. As the main area of tropical-Pacific convection changes from a zonally extended SPCZ in LGM to a more zonally confined region in the western Pacific in GHS, anomalous convective activity moves from a zonal band south of the Equator to a narrower, near-Equatorial region around the dateline in GHS. As a result, the maximum SST anomalies are widely separated from the maximum precipitation anomalies in LGM, while they are nearly co-located in GHS. This contributes to increased precipitation anomalies, and the wind anomalies become more confined, more coherently zonal in direction, and more symmetric about the Equator, with a larger El Niño-related reduction in the magnitude of (Easterly) zonal windstress over the central Equatorial Pacific.

Figure 3 shows diagnostics introduced by Timmermann et al. (1999) as a proxy for the strength of the coupled feedbacks responsible for growth of the ENSO mode. Between CTL and GHS there is an increase in "atmospheric sensitivity" (the covariance of zonal-average Equatorial windstress and NINO3.4 SST anomalies, divided by the variance of NINO3.4 SSTa). A similar behaviour is found in the transient greenhouse-forced simulation (orange curve in Fig. 4), which also displays an increase in frequency and a Westward displacement of the ENSO SST pattern (Toniazzo, 2002), and has a steadily increasing atmospheric sensitivity index with a fairly stable oceanic sensitivity index. The differences in atmospheric response between CTL and LGM are less clear-cut; LGM tends to have larger upwelling anomalies in the East Pacific favouring the growth of SSTa there (Toniazzo, 2005[4]).

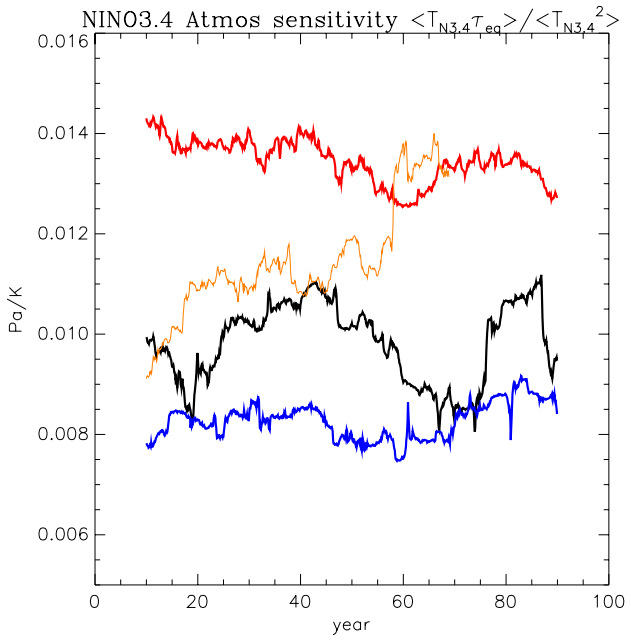

Fig. 3. Atmospheric sensitivity indices (after Timmermann et al. 1999) for the three HadCM3 integrations. The orange curve represents an integration joining CTL and GHS with an yearly 2% increase in CO_2.

All HadCM3 integrations show some evidence of Westward propagating SST anomalies in the growing stages of positive ENSO anomalies, suggesting a significant role of the local advection-upwelling "SST mode", regulated by anomalous advection and upwelling rather than subsurface ocean temperature anomalies (Neelin et al., 1998), during an El Niño. However, differences can be seen in the feedback provided by surface fluxes in response to SST anomalies (Fig. 4). Significant damping from surface-flux anomalies starts occurring in winter, when convective activity is sufficiently encouraged near the SSTa's, and with reduced amplitude in LGM which has the least convection over the Equator. In GHS, however, large surface-flux anomalies are essentially co-located with the maximum wind anomaly already in Autumn, and provide stronger damping. Such changes in behaviour are related to the spatial locations and seasonality of the climatological convective areas for each simulation.

2.2 Changes in mean-climate properties and their likely impacts on ENSO

The main differences in oceanic and atmospheric mean state and annual cycle over the tropical Pacific are highlighted in Table 1. The reader is referred to Toniazzo (2005)[4] for details. Many changes are associated to the changed location and activity of the Pacific ITCZs, as well as changed climatological surface fluxes.

Table 1 also lists the impacts that such changes may have on the ENSO, as predicted by theoretical or modeling work based in ICMs (Neelin et al., 1998). The two last entries on the right-hand side of the table refer to the changes in feedbacks seen in the previous section (atmospheric sensitivity and surface-flux damping) that cannot be directly related to climate-mean properties with C-Z type ICMs; they roughly correspond to the coupling parameter μ and the damping parameter ϵ_T of Jin and Neelin (1993), respectively.

This comparison with existing ENSO models suggests an increasing role of surface processes in regulating the evolution of SST anomalies in GHS. However, the picture that emerges from direct analysis of the GCM (Toniazzo, 2005[4]) is more complex and to understand the relative contribution of each change in the climatology to the changes in ENSO further modelling is needed. In particular, the role of changed atmospheric convection patterns, which appear to provide a stronger coupling, depends on annual-mean and seasonal ocean-atmospheric feedbacks that cannot be captured with "traditional" C-Z models.

The smaller ENSO shift between LGM and CTL is more complex and the simplified modelling framework less helpful for the identification of possible mechanisms. The type of analysis carried out by An et al. (2004), based on linear analysis of a Cane-Zebiak ICM, can provide useful insight, but it would be desirable to complement it with spatially resolved coupled dynamical modelling. For example, the eastward ENSO pattern shift may be related with the relatively cool tropical Atlantic and the strengthened Atlantic meridional overturning in a way consistent with the results of Zhang and Delworth (2005). We attempt to address these issues with the help of a slightly more complex ICM.

3 Analogue sensitivity experiments with an Intermediate Coupled Model

3.1 The model

The ICM we have adopted comprises three components, shortly described as follows:

Ocean: 2-active-layer, spherical, shallow water model for the Tropical Pacific (30 S–30 N) basin (Wang, Li and Chan, 1995)

Atmosphere: linear baroclinic free troposphere and barotropic mixed layer, β-plane, shallow-water, Tropical atmosphere, with a LW radiative transfer scheme and parametrised surface heat fluxes and convective heating of the free troposphere (Wang and Li, 1993; Fu and Wang, 1999);

Coupling scheme: direct SST forcing of atmosphere-model mixed layer; direct windstress forcing of ocean model; ocean surface-fluxes from advective-diffusive well-mixed atmospheric surface-layer model (Betts, 1976; Seager et al., 1995);

The atmospheric component is formulated as an anomaly model, and depends on an assumed monthly climatology

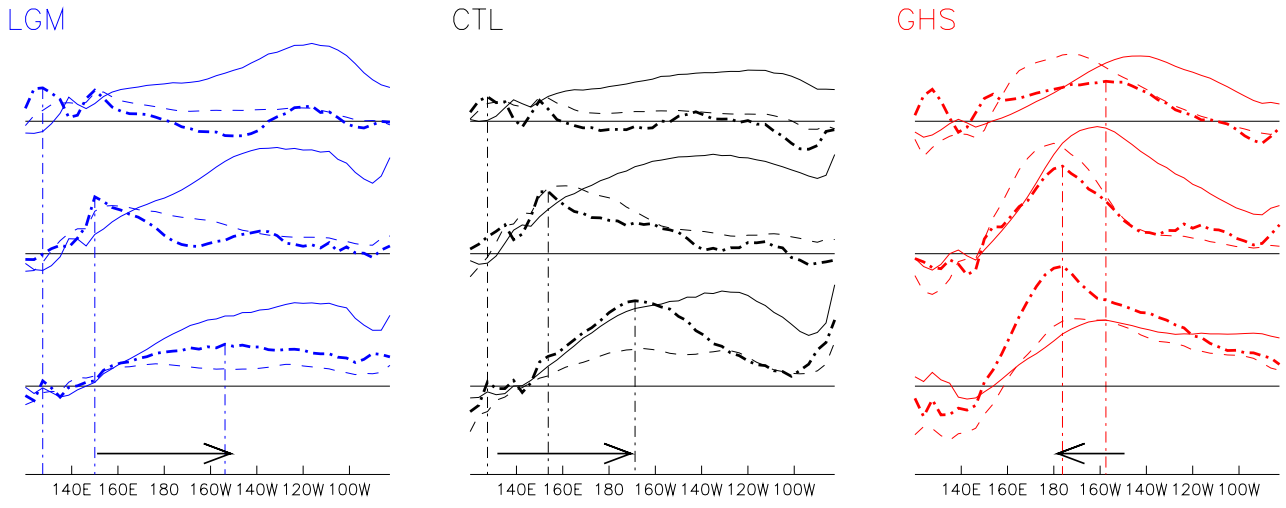

Fig. 4. Surface flux anomalies normalised to the NINO3.4 SST anomaly (W/m^2/°C, the heavy dash-dotted line), SST anomalies (thin solid lines) and precipitation anomalies (thin dashed lines), split into averages for the growing stage (MJJA, first graph from the top in each panel), saturating stage (SOND, second graph from the top), and decaying stage (JFMA, graphs at the bottom) of an El Niño event.

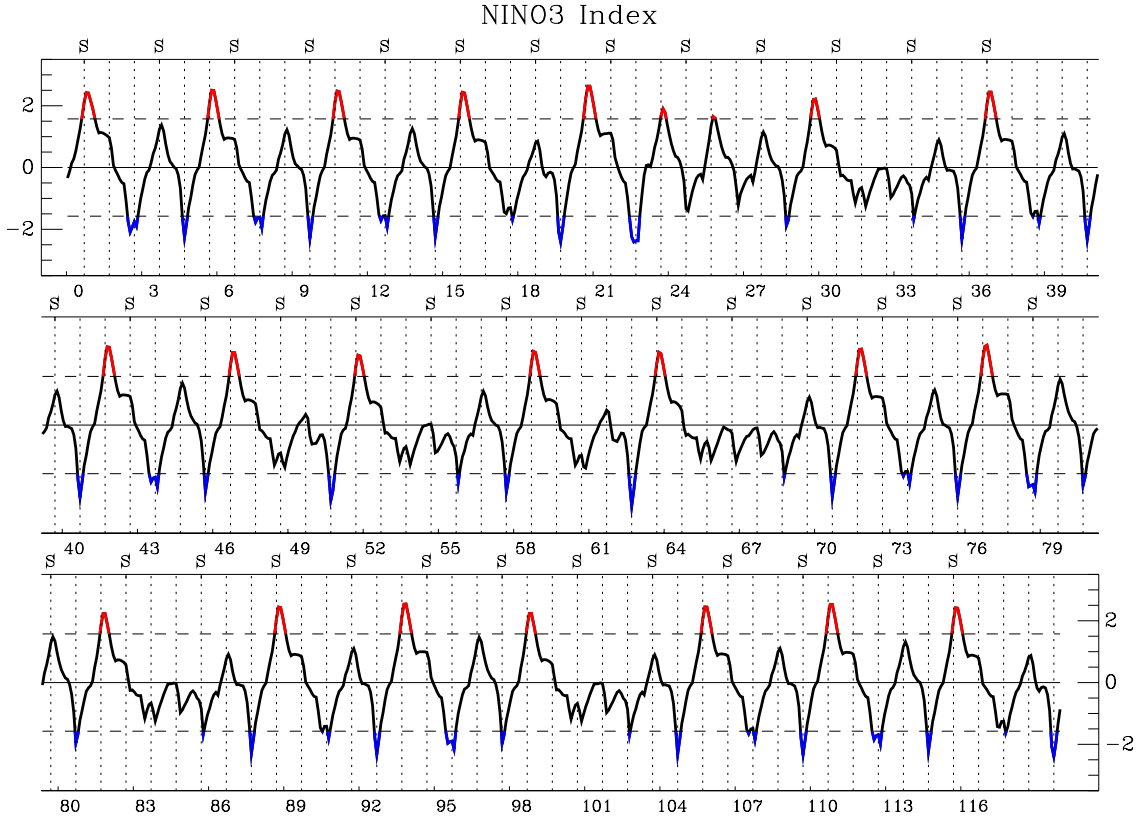

Fig. 5. NINO3 index in a 120-year integration of the ICM.

specifying surface temperature and humidity outside the tropical Pacific (where the ocean model provides these quantities), a background lapse rate or stability parameter, cloud fraction and cloud-top temperature (which largely determine the location of climatological convective areas), and solar forcing. The coupling scheme also assumes a climatology of near-surface air temperature and winds to provide the boundary conditions for the advective-diffusive mixed-layer

Table 1. Summary of the differences in climatology between the three HadCM3 integrations and their expected impacts on ENSO according to ICM modelling work. The last row indicates whether we find agreement with results from our analysis of the HadCM3 integrations.

	Mean Zonal Windstress	Annual cycle of zonal windstress	Meridional SST gradient	Ocean Surface Stability	Depth of thermocline	ΔT across thermocline	Atmospheric sensitivity (μ)	Surface-flux damping (ϵ_T)
CTL-LGM	+ in West and central Pacific, − in east Pacific	weakening; winter maximum +, late-summer maximum −	−	∼	∼ in W, + in E	∼	+ (but not at all times)	+
GHS-CTL	−	annual component +, shorter period of strong Easterlies	−	+	−	−	+	+
ENSO response:								
Amplitude A								
CTL-LGM:	−	likely −	likely +	∼	∼	∼	+	−
GHS-CTL:	∼	sharper phase-locking	likely +	probably +	−	+	+	−
Frequency ν								
CTL-LGM:	+	∼	likely −	∼	∼	∼	− (+)	+
GHS-CTL:	−	∼	likely −	probably +	+	−	− (+)	+
References	Fedorov and Philander (2001), Wang and An (2002)	Jin et al. (1996), Chang et al. (1995)	An et al. (2004)	Jin and Neelin (1993)	Fedorov and Philander (2001); An et al. (2004)	Fedorov and Philander (2001)	Jin and Neelin (1993)	Jin and Neelin (1993)
Comments	CTL-LGM: analogous but inverse change as in pre-1976 to post-1976. GHS-CTL: A change depends on regime.		tends to act as a damping	like ICM parameter δ_s, may favour SST modes with generally higher ν; A generally ↗	if thermocline feedback is important, ν ↗ and A ↘; ν ↘ only in extreme SST regime		ν response depends on regime: generally − for mixed modes, + only in fast-wave limit	general, see e.g. Eq.(2.6) in Jin 1997.
Present analysis:	CTL-LGM: yes GHS-CTL: no	Yes	No	ν: yes A: compensation?	ν: yes	No	ν: no A: compensation?	ν: yes

equations. The atmosphere-ocean and the ocean-atmosphere coupling schemes are not fully consistent; for example anomalous SSTs are not damped by the atmospheric radiation scheme.

A number of parameters are further needed to completely specify the model. It exceeds the scope of this presentation to discuss them all, and the interested reader is referred to the articles referenced above. Below we give two examples of parameter perturbation, but first we'll discuss the ICM's ENSO.

3.2 ENSO in the ICM and proposed sensitivity studies

Given an initial windstress anomaly, the model produces a self-sustained ENSO cycle with some irregularities, a period between 2 and 4 years, and an amplitude of around 1.5 Kelvin. An example of the NINO3 index time-series is shown in Fig. 5. The amplitude varies decadally, but as is common for ICMs the seasonal locking is very tight, with warm anomalies always peaking in November, and cold anomalies in September.

The evolution of SST anomalies (not shown) in the standard set-up shows strong Westward-propagation, suggesting a dominant SST mode (Jin and Neelin, 1993). Also, SST anomalies in the West appear to be rather persistent, suggesting insufficient flux-damping. In the present two-way coupling set-up, thermal SST damping is mainly evaporative. The ICM thus needs some adjustment in the parameters and in some parts of its formulation to better tune the balance of ENSO feedbacks towards the observed one. Nevertheless, it demonstrates the capability of producing a reasonable, self-sustained ENSO, consistent with its own oceanic seasonal

cycle, that can be used for sensitivity studies of the kind of Fedorov and Philander (2001).

As a preliminary study we have attempted to use sensitivity experiments with the ICM for comparison with our results from the analysis of the HadCM3 integrations. In one experiment, the inert-layer temperature T_0 below the ocean thermocline is increased from 10 to 14°C. This is analogous to reducing ΔT in C-Z type models (Fedorov and Philander, 2001), and emulates the reduced stability of the thermocline in the GHS integration of HadCM3 compared to CTL. The changes in oceanic climatology are qualitatively similar to those between GHS and CTL, with warmer SSTs related with reduced cooling from upwelling, weakened zonal and meridional SST gradients and reduced zonal windstress. The effect on ENSO is a larger thermocline feedback, consistent with the GCM analysis (Toniazzo, 2005[4]) and with previous results (Fedorov and Philander, 2001), resulting in a larger amplitude and a lower frequency. In HadCM3, the reduced stability of the thermocline in GHS is clearly not the dominant influence on ENSO, given that the frequency of ENSO is higher. From Table 1, we might expect increased damping or increased surface stability below the ocean mixed-layer to increase the frequency. We have tried ICM integrations with increased surface-flux dissipation (atmospheric LW opacity reduced by 10%) and with reduced momentum coupling between the mixed-layer and the thermocline (vertical turbulent mixing coefficient reduced by $1/3$). In the first case, we find increased ENSO frequency, and reduced amplitude, consistently, again, with Table 1. The second perturbation, however, also entails significant changes to the climatology, with an increase in zonal windstress. From Table 1, this tends to oppose the effects of increased surface stability on the ENSO, and the resulting changes are indeed very small. Although these results are still preliminary and a better experimental design is clearly needed, such complex dependencies between the sensitivity of ENSO-related processes and the mean climatology highlight the need for self-consistency in dynamical sensitivity studies of the ENSO based on ICMs.

4 Conclusions

The changes in the ENSO produced by HadCM3 in different equilibrium climate integration can be partly attributed to changes in the the sensitivity of the lower atmosphere to SST forcing. Such result appears consistent with previous work (Guilyardi et al., 2004). While the total variance in SSTa does not change significantly, in progressively warmer climates the frequency increases and the largest SSTa move towards the Central Equatorial Pacific. These results however are likely to be model-dependent, and their robustness is uncertain, so that better understanding in terms of individual ENSO-related processes is necessary. Comparison with published work based on intermediate coupled models (ICMs), mainly of the type pioneered by Cane and Zebiak (1985), shows that the mean-climate changes can have contrasting effects on the amplitude and the frequency of the ENSO, so that the final result depends on the balance between different mechanisms, and may be sensitive to inconsistencies between mean-state changes and changes in the ENSO feedbacks.

To address such issues, we have started working on experiments with an ICM borrowed from IPRC/SOEST at Hawaii University, that has a better representation of the atmospheric component and produces its own ocean climatology. Our preliminary results so far are consistent with earlier work (Fedorov and Philander, 2001), but also stress the importance of self-consistency between oceanic and atmospheric changes for the ENSO.

We are currently trying to achieve some desirable improvement to the ICM, in particular in the balance of thermocline versus surface coupled feedbacks and in the treatment of radiation fluxes. Furthermore, we are searching for an analytically tractable approximation for the ICM atmospheric parameterisations in order to permit formal stability analysis. We hope to eventually construct ICM analogues of the GCM ENSO-climate sensitivities and to use them to better understand and assess the GCM performance itself.

Acknowledgements. I am grateful to B. Wang for providing me with the complete code of the ICM. I wish to thank M. Collins, H. Djikstra, G. van Oldenborgh and A. Wittenberg for interesting, friendly and stimulating discussions at the "1st A. von Humboldt" conference in Guayaquil. I also thank C. Hewitt for providing the data from the HadCM3 LGM integration to me.

Edited by: P. Fabian and J. L. Santos
Reviewed by: two anonymous referees

References

An, S.-I., Timmermann, A., Bejarano, L., Jin, F.-F., Justino, F., Liu, Z., Tudhope, A.W.: Modeling evidence for enhanced El Niño-Southern Oscillation amplitude during the last glacial maximum, Palaeoceanography, 19 (4), PA4009, 2004.

Betts, A. K.: Modeling subcloud layer structure and interaction with a shallow cumulus layer, J. Atmos. Sci., 33, 2363–2382, 1976.

Cane, M. A. and Zebiak, S. E.: A theory for El Niño and the Southern Oscillation, Science, 228, 1084–1087, 1985.

Chang, P., Link, Ji, Wang, B., Li, T.: Interactions between the Seasonal Cycle and El Niño-Southern Oscillation in an Intermediate Coupled Ocean-Atmosphere Model, J. Atmos. Sci., 52/13, 2353-2372, 1995.

Collins, M. and The CMIP Modelling Groups (BMRC (Australia), CCC (Canada), CCSR/NIES (Japan), CERFACS (France), CSIRO (Australia), MPI (Germany), GFDL (USA), GISS (USA), IAP (China), INM (Russia), LMD (France), MRI (Japan), NCAR (USA), NRL (USA), Hadley Centre (UK), YNU (South Korea)): El Niño- or La Niña-like climate change?, Clim. Dyn., 24, 89–104, 2005.

Dijkstra, H. A. and Neelin, J. D.: On the attractors of an intermediate coupled ocean-atmopshere model, Dyn. Atmos. Oc., 22, 19–48, 1995.

Fedorov, A. V. and Philander, S. G.: A stability analysis of tropical ocean-atmosphere interactions: bridging measurements and theory for El Niño, J. Clim., 14, 3086–3101, 2001.

Fu, X. and Wang, B.: The role of longwave radiation and boundary layer thermodynamics in forcing tropical surface winds, J. Clim., 12, 1049–1069, 1999.

Guilyardi, E., Gualdi, S., Slingo, J., Navarra, A., Delecluse, P., Cole, J., Madec, G., Roberts, M., Latif, M., and Terray, L.: Representing El Niño in coupled ocean-atmopshere GCMs: the dominant role of the atmopsheric component, J. Clim., 17, 4623–4629, 2004.

Hewitt, C. D., Broccoli, A. J., Mitchell, J. F. B., and Stouffer, E. J.: A coupled model study of the last glacial maximum: was part of the North Atlantic relatively warm?, Geophys. Res. Lett., 28 (8), 1571–1574, 2001.

Hewitt, C. D., Stouffer, R. J., Broccoli, A. J., Mitchell, J. F. B., and Valdes, P.J.: The effect of ocean dynamics in a coupled GCM simulation of the last glacial maximum, Clim. Dyn., 20, 203–218, 2003.

Jin, F.-F.: An equatorial recharge paradigm for ENSO, I, Conceptual model, J. Atmos. Sci., 54, 811–929, 1997.

Jin, F.-F. and Neelin, J. D.: Modes of interannual tropical ocean-atmosphere interaction – a unified view, I, Numerical results, J. Atmos. Sci., 50, 3477–3503, 1993.

Jin, F.-F., Neelin, J. D., and Ghil, M.: El Niño/Southern Oscillation and the annual cycle: subharmonic frequency locking and aperiodicity, Physica D, 98, 442–465, 1996.

Neelin, J. D. and Dijkstra, H. A.: Ocean-atmosphere interaction and the tropical climatology: Part I: The dangers of flux correction, J. Clim., 8, 1325–1342, 1995.

Neelin, J. D., Battisti, D. S, Hirst, A. C., Jin, F.-F., Wakata, Y., Yamagata, T., and Zebiak, S. E.: ENSO theory, J. Geophys. Res., 103, 14 261–14 290, 1998.

Peltier, W. R.: Ice-age Paleotopography, Science, 265, 195–201, 1994.

Seager, R., Blumenthal, M. B., and Kushnir, Y.: An advective atmospheric mixed layer model for ocean modeling purposes: global simulation of surface heat fluxes, J. Clim., 8, 1951–1964, 1995.

Sun, D.-Z.: A possible effect of an increase in the Warm-Pool SST on the magnitude of El Niño warming, J. Clim., 16/2, 185–205, 2003.

Thorpe, T.: Report on the Possible Long-Term Global Climate Response to a Stabilisation of CO2 at 4x Pre-Industrial Levels, Hadley Centre report to the UK Department of Environment, Fisheries and Rural Affairs, 2004.

Timmermann, A., Oberhuber, J., Bacher, A., Esch, M., Latif, M., and Roeckner, E.: Increased El Niño frequency in a climate model forced by future greenhouse warming, Nature, 398, 694–697, 1999.

Toniazzo, T.: Report on ENSO in a HadCM3 warming scenario, Hadley Centre report to the UK Department of Environment, Fisheries and Rural Affairs, 2002.

Wang, B. and Li, T.: A simple tropical atmosphere model of relevance to short-term climate variations, J. Atmos. Sci., 50/2, 260–284, 1993.

Wang, B., Li, T., and Chang, P.: An intermediate model of the tropical Pacific ocean, J. Phys. Oceanogr., 25, 1599–1616, 1995.

Wang, B. and An, S. I.: A mechanism for decadal changes of ENSO behaviour: roles of background wind changes, Clim. Dyn., 18, 475–486, 2002.

Zhang, R. and Delworth, T. L.: Simulated tropical response to a substantial weakening of the Atlantic thermohaline circulation, J. Clim., 18, L1853–1860, 2005.